



**HAL**  
open science

# Dominant Role of Quantum Anharmonicity in the Stability and Optical Properties of Infinite Linear Acetylenic Carbon Chains

Davide Romanin, Lorenzo Monacelli, Raffaello Bianco, Ion Errea, Francesco Mauri, Matteo Calandra

► **To cite this version:**

Davide Romanin, Lorenzo Monacelli, Raffaello Bianco, Ion Errea, Francesco Mauri, et al.. Dominant Role of Quantum Anharmonicity in the Stability and Optical Properties of Infinite Linear Acetylenic Carbon Chains. *Journal of Physical Chemistry Letters*, 2021, 12 (42), pp.10339 - 10345. 10.1021/acs.jpcclett.1c02964 . hal-03407561

**HAL Id: hal-03407561**

**<https://hal.sorbonne-universite.fr/hal-03407561>**

Submitted on 29 Oct 2021

**HAL** is a multi-disciplinary open access archive for the deposit and dissemination of scientific research documents, whether they are published or not. The documents may come from teaching and research institutions in France or abroad, or from public or private research centers.

L'archive ouverte pluridisciplinaire **HAL**, est destinée au dépôt et à la diffusion de documents scientifiques de niveau recherche, publiés ou non, émanant des établissements d'enseignement et de recherche français ou étrangers, des laboratoires publics ou privés.

This document is confidential and is proprietary to the American Chemical Society and its authors. Do not copy or disclose without written permission. If you have received this item in error, notify the sender and delete all copies.

## Dominant Role of Quantum Anharmonicity in the Stability and Optical Properties of Infinite Linear Acetylenic Carbon Chains

Journal:	<i>The Journal of Physical Chemistry Letters</i>
Manuscript ID	jz-2021-02964d.R2
Manuscript Type:	Letter
Date Submitted by the Author:	12-Oct-2021
Complete List of Authors:	Romanin, Davide; Institut des NanoSciences de Paris, CNRS Monacelli, Lorenzo; Universita degli Studi di Roma La Sapienza, Physics Department Bianco, Raffaello; Centro de Fisica de Materiales Errea, Ion; Centro de Fisica de Materiales Mauri, Francesco; University of Rome La Sapienza, Department of Physics Calandra, Matteo; Università degli Studi di Trento, Departement of Physics

SCHOLARONE™  
Manuscripts

# Dominant Role of Quantum Anharmonicity in the Stability and Optical Properties of Infinite Linear Acetylenic Carbon Chains

Davide Romanin,<sup>\*,†</sup> Lorenzo Monacelli,<sup>‡</sup> Raffaello Bianco,<sup>¶</sup> Ion Errea,<sup>¶,§</sup>

Francesco Mauri,<sup>‡</sup> and Matteo Calandra<sup>\*,||,†</sup>

<sup>†</sup>*Sorbonne Université, CNRS, Institut des Nanosciences de Paris, UMR7588, F-75252, Paris, France*

<sup>‡</sup>*Dipartimento di Fisica, Università di Roma La Sapienza, Piazzale Aldo Moro 5, I-00185 Roma, Italy*

<sup>¶</sup>*Centro de Física de Materiales (CSIC-UPV/EHU), Manuel de Lardizabal pasealekua 5, 20018 Donostia-San Sebastián, Basque Country, Spain*

<sup>§</sup>*Fisika Aplikatua 1 Saila, Gipuzkoako Ingeniaritza Eskola, University of the Basque Country (UPV/EHU), Europa Plaza 1, 20018, Donostia San Sebastián, Basque Country, Spain*

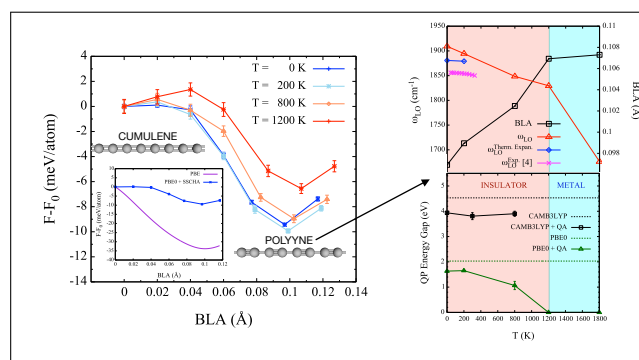
<sup>||</sup> *Department of Physics, University of Trento, Via Sommarive 14, 38123 Povo, Italy*

E-mail: romanin@insp.jussieu.fr; m.calandrabuonaura@unitn.it

## Abstract

Carbyne, an infinite-length straight chain of carbon atoms, is supposed to undergo a second order phase transition<sup>1</sup> from the metallic bond-symmetric cumulene  $(=C=C=)_\infty$  towards the distorted insulating polyynic chain<sup>2</sup>  $(-C\equiv C-)_\infty$  displaying bond-length alternation. However, recent synthesis of ultra long carbon chains ( $\sim 6000$  atoms)<sup>3-5</sup> did not show any phase transition and detected only the polyynic phase, in agreement with previous experiments on capped finite carbon chains.<sup>6,7</sup> Here, by performing first principles calculations, we show that quantum-anharmonicity reduces the energy gain of the polyynic phase with respect to the cumulene one by 71%. The magnitude of the bond-length alternation increases by increasing temperature, in stark contrast with a second order phase transition,<sup>1</sup> confining the cumulene-to-polyynic transition to extremely high and unphysical temperatures. Finally, we predict that a high temperature insulator-to-metal transition occurs in the polyynic phase confined in insulating nanotubes with sufficiently large dielectric constant due to a giant quantum-anharmonic bandgap renormalization.

## Graphical TOC Entry



1  
2  
3 Charge density waves (CDW) are broken symmetry states in solids in which the crys-  
4 tal acquires a periodic modulation of a given wavevector at low temperature. They are  
5 ubiquitous as they occurs in many different systems ranging from high- $T_c$  superconduc-  
6 tors,<sup>8</sup> transition metal dichalcogenides,<sup>9</sup> 2D materials<sup>10–12</sup> and one dimensional systems.<sup>2,13</sup>  
7 The understanding of this phenomenon is difficult as it is determined by the interplay of  
8 three effects: the electron-electron interaction, the electron-phonon coupling and quantum  
9 anharmonicity. On a general basis, the electron-phonon interaction enhances the tendency  
10 towards CDW while quantum anharmonicity suppresses it.<sup>14–16</sup> Nevertheless, few estimates  
11 of the magnitude of quantum anharmonicity are present in literature<sup>14–16</sup> mostly because of  
12 its non-perturbative nature. Moreover, in the case of light atoms, the quantum nature of  
13 the ions is crucial and difficult to treat with conventional density functional theory (DFT)  
14 <sup>17</sup> or standard molecular dynamics approaches.

15  
16  
17  
18  
19  
20  
21  
22  
23  
24  
25  
26  
27 Linear acetylenic carbon, or carbyne,<sup>18</sup> is considered the physical realization of a one  
28 dimensional CDW. Therefore, the understanding of the finite temperature phase diagram of  
29 this system and the comprehension of the mutual role of the relevant interactions (electron-  
30 phonon, electron-electron and quantum anharmonicity) is of paramount importance. His-  
31 torically,<sup>1,2</sup> the cumulene-to-polyyne transition was attributed to the electron-phonon inter-  
32 action and the perfect nesting condition at  $2k_F$  in cumulene, leading to a divergence in the  
33 real part of the charge-charge response function at  $T = 0$  K. This consequent large single  
34 particle energy gain due to gap opening should stabilize the polyynic phase. However, this  
35 hypothesis, valid in the small displacements regime, is unlikely.

36  
37  
38  
39  
40  
41  
42  
43  
44  
45 Several density functional theory based calculations (neglecting quantum anharmonicity)  
46 showed a band-gap opening larger than 2 eV (see Tab. 1), with a total energy gain of the  
47 polyynic phase with respect to the cumulene one smaller than 150 meV.<sup>19</sup> Moreover, the  
48 bond-length alternation (BLA), defined as the length difference between the single ( $r_1$ ) and  
49 the triple ( $r_3$ ) bonds of polyynic, is found to be substantial and ranging between 0.09 –  
50 0.14 Å (corresponding to 7 – 10% of the average bond length of polyynic). These structural  
51  
52  
53  
54  
55  
56  
57  
58  
59  
60

1  
2  
3 distortions from the ideal cumulene phase are definitely not in the small displacement limit.  
4  
5 Still one would expect that raising temperature the BLA should progressively reduce, as  
6  
7 it happens in a second order phase transition, and the cumulene phase becomes stable at  
8  
9 some critical temperature  $T_{CDW}$ . This argument, however, does not account for quantum-  
10  
11 anharmonicity, whose magnitude and temperature dependence are still largely unexplored in  
12  
13 literature. Moreover, the experimental data are in stark disagreement with the occurrence  
14  
15 of a cumulene-to-polyyne phase transition as at any temperature cumulene observations are  
16  
17 very rare (and mostly related to strain and charging effects<sup>20-22</sup>), while polyyne has been  
18  
19 obtained either in relatively small (up to  $\sim 44$  atoms) end-capped chains<sup>6,7,23</sup> or through  
20  
21 encapsulation in single-,<sup>24,25</sup> double-<sup>4,26</sup> and multi-walled<sup>27</sup> carbon nanotubes, with chains  
22  
23 as long as  $\sim 6000$  atoms.

24  
25 In this work we investigate the ground state and the CDW transition of infinite carbon  
26  
27 chains by using hybrid functionals, self-consistent GW, the Bethe-Salpeter equation and by  
28  
29 including quantum anharmonicity within the Stochastic Self-Consistent Harmonic Approx-  
30  
31 imation (SSCHA).<sup>17,28-30</sup> We show that quantum anharmonicity completely reshapes the  
32  
33 stability of the different carbyne phases, reducing the energy difference between the polyyne  
34  
35 and cumulene phase by 71%. Even more surprisingly, we show that the BLA *increases* by  
36  
37 *increasing* temperature, the opposite of what is expected in a second order phase transi-  
38  
39 tion. Finally, we demonstrate that quantum-anharmonic effects on optical properties are  
40  
41 extremely large and strongly temperature dependent.

42  
43 In order to do so, density functional theory (DFT) calculations are performed both with  
44  
45 the plane-wave pseudopotential method, using the Perdew-Burke-Ernzerhof (PBE) exchange-  
46  
47 correlation (xc) functional and Quantum ESPRESSO,<sup>31,32</sup> and with localized gaussian ba-  
48  
49 sis, using both the PBE0 and CAMB3LYP hybrid xc functionals and CRYSTAL.<sup>33,34</sup> In  
50  
51 the Quantum ESPRESSO code we use a norm-conserving pseudopotential, while in the  
52  
53 CRYSTAL code we use the triple- $\xi$ -polarized Gaussian type basis set.<sup>35</sup> Quantum anhar-  
54  
55 monicity is taken into account via the stochastic self-consistent harmonic approximation  
56  
57  
58  
59  
60

(SSCHA),<sup>17,28–30</sup> for which we use the CRYSTAL<sup>33,34</sup> code as force engine: forces and energies are computed on supercells with 20 atoms per unit cell, containing the unstable phonon mode. Optical properties of the distorted phase are computed within the self-consistent GW approximation on eigenvalues only (evGW) using the Yambo<sup>36,37</sup> code within the plasmon-pole approximation.<sup>38</sup> Excitonic effects for the freestanding carbon chain are then evaluated by solving the Bethe-Salpeter<sup>39,40</sup> equation (BSE) on top of the evGW band structure. More details concerning computational methods can be found in the Supporting Informations.

A large number of first-principles calculations have been performed on linear carbon chains of both finite and infinite size, however almost all of them neglect quantum anharmonicity and its temperature dependent effects as well as its interplay with electron-electron interaction. The calculated quasiparticle band gap as well as the BLA value are strongly dependent on the assumptions employed to model electron-electron interaction<sup>41–45</sup> (Tab. 1). The best results with respect to more accurate treatments of electronic correlation (e.g. quantum Monte Carlo<sup>45</sup> or RPA<sup>46</sup>) for carbyne in vacuum are obtained via DFT and partial inclusion of the exact exchange from Hartree Fock (HF), as parametrized in hybrid functionals with unscreened long range exchange such as CAMB3LYP<sup>42–44</sup> (see the inset of Fig. 3 (a) and Sec. S4 in the SI). However, even if the PBE0 hybrid functional gives a slightly reduced BLA in vacuum, its value is very close to that of very long carbon chains inside the dielectric environment of the carbon nanotube<sup>46</sup> (see Tab. 1, as well as Sec. S4 in the SI). Indeed, the BLA is expected to strongly depend on the environment around the carbyne chain. For this reason, and to better compare with experiments, in the following we adopt the CAMB3LYP functional to model carbyne in vacuum and PBE0 to describe carbyne in the presence of the dielectric environment of the nanotube.<sup>47</sup>

**Table 1: Structural, optical and vibrational properties of carbyne for different exchange correlation functionals with and without quantum anaharmonic (QA) effects. The column  $n$  shows if the calculation is obtained on an infinite system with periodic boundary conditions (PBC) or on chains of finite size of length  $n$ . The subsequent four columns are used to describe the accuracy of the computational methods:  $MF$  refers to a mean-field approach,  $X$  and  $C$  are used to signal a more accurate treatment for electronic exchange interaction and correlation respectively, while  $QA$  indicates if quantum nuclear fluctuations are taken into account. The polyyne lattice parameter is labeled  $2c$ , while  $r_1$  and  $r_3$  are the single and triple bond lengths, respectively. The bond length alternation (BLA) is defined as  $r_3 - r_1$ . Finally  $\Delta E$  and  $\omega_{LO}$  represents the quasiparticle energy band-gap and the longitudinal optical frequency at the zone center, respectively.**

Method	n	MF	X	C	QA	$2c$ (Å)	$r_1$ (Å)	$r_3$ (Å)	BLA (Å)	$\Delta E$ (eV)	$\omega_{LO}$ (cm <sup>-1</sup> )
This work											
DFT-PBE0	PBC	•	•			2.534	1.3156	1.2183	0.0973	2.03	1986.57
DFT-CAMB3LYP	PBC	•	•			2.526	1.3286	1.1973	0.1313	4.39	2277.22
DFT-PBE0 + QA	PBC	•	•		•	2.534	1.3154	1.2185	0.0969	1.63 (0 K)	1909.3
DFT-CAMB3LYP + QA	PBC	•	•		•	2.526	1.3304	1.1955	0.1348	3.94 (0 K)	2226.5
evGW@PBE0	PBC		•	•		2.534	1.3154	1.2185	0.0969	3.21	-
evGW@CAMB3LYP	PBC		•	•		2.526	1.3304	1.1955	0.1348	4.32	-
Literature											
DMC <sup>45</sup>	PBC		•	•		2.5817(9)	1.359(2)	1.223(2)	0.136(2)	3.4(1)	2084(5)
DMC+ZPE on $\Delta E$ <sup>45</sup>	PBC		•	•		2.5817(9)	1.359(2)	1.223(2)	0.136(2)	3.3(0)	-
RPA (vacuum) <sup>46</sup>	PBC	•	•	•		2.590	1.36	1.23	0.129	-	2000
RPA (nanotube) <sup>46</sup>	PBC	•	•	•		2.590	1.3405	1.2495	0.091	-	1614
HF <sup>42</sup>	72	•	•			-	-	-	0.183	8.500	-
MP2 <sup>42</sup>	40		•	•		-	-	-	0.060	5.541	-
MP2 <sup>41</sup>	PBC		•	•		2.554	1.337	1.217	0.120	-	-
CCSD(T) <sup>48</sup>	36		•	•		-	-	-	0.125	-	2090
CCSD(T) <sup>41</sup>	PBC		•	•		2.565	1.358	1.207	0.151	-	-
DFT-LDA <sup>41</sup>	PBC	•				2.532	1.286	1.246	0.040	-	-
DFT-PBE <sup>45</sup>	PBC	•				2.565	1.300	1.265	0.035	-	-
DFT-HSE06 <sup>45</sup>	PBC	•	•			2.56	1.323	1.237	0.086	-	-
DFT-B3LYP <sup>42</sup>	72	•	•			-	-	-	0.088	1.487	-

The role played by quantum effects on the BLA is still undisclosed. The zero point energy contribution to the free energy is larger than the energy gain between the cumulene and polyyne structures.<sup>19</sup> The only existing calculation performed by including to some extent quantum anharmonicity confirms this argument and shows that polyyne is not anymore stable if a semilocal functional (PBE) is used as force engine,<sup>19</sup> in qualitative disagreement with experiments and again pointing to the crucial role of quantum anharmonicity and electron-electron interaction. However, PBE is known to be largely inaccurate for carbyne as it underestimates the BLA by  $\approx 75\%$  with respect to quantum Monte Carlo simulations (Tab. 1).

The relative stability of the cumulene and polyne phases inside CNTs as a function of temperature can be determined by calculating the quantum free energy in the SSCHA as a function of the BLA (Fig. 1 and Sec. S2 in the SI) using PBE0. At  $T = 0$ , cumulene is unstable towards polyne. The quantum total energy difference is  $\approx 9$  meV/atom, while the classical total energy difference (reported in the inset of Fig. 1) is  $\approx 34$  meV/atom. The comparison between these two results highlights the crucial role of quantum anharmonicity leading to a 71% suppression of the energy gain by the distortion (a reduction of 25 meV/atom). If quantum anharmonicity is neglected, the phase stability of polyne is significantly overestimated.

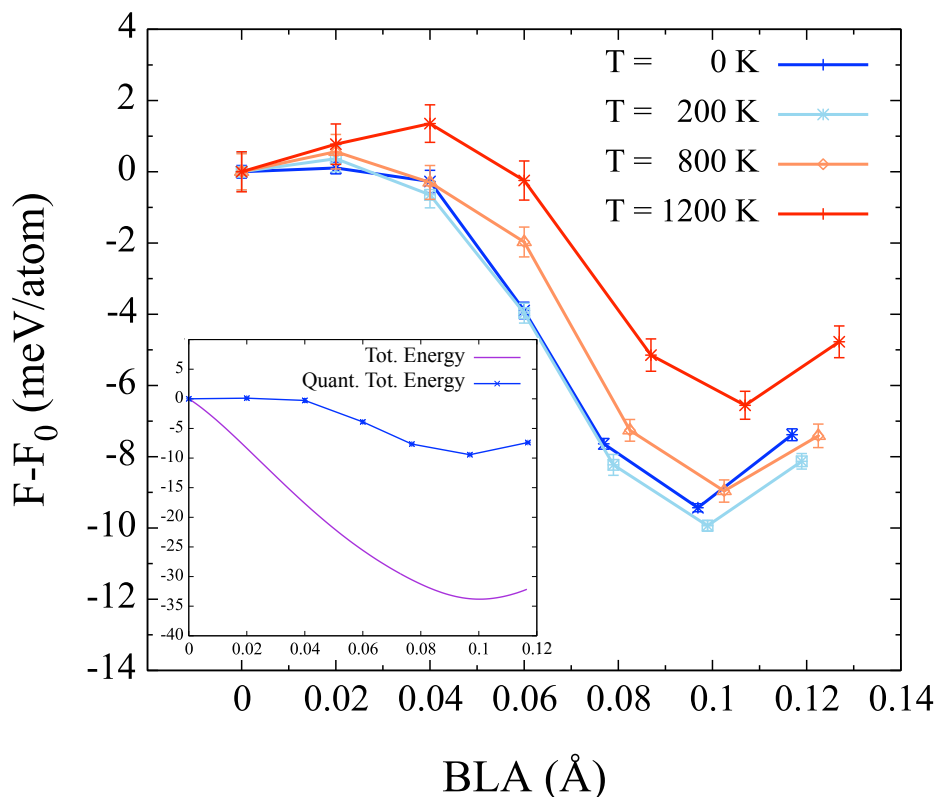


Figure 1: **First-order phase transition in carbyne.** a) Quantum anharmonic free energy difference per carbon atom between the polyne and cumulene phases as a function of the bond length alternation (BLA) and temperature. The inset shows the comparison between the total energy difference and the quantum free energy difference at  $T = 0$  between the two phases as a function of the BLA.

As temperature is raised, cumulene becomes metastable, with a small local minimum in

the quantum free energy at BLA= 0 (Fig. 1) that occurs for  $T > T_P \approx 75\text{K}$  (see Sec. S2.4 in SI for the estimate of  $T_P$ ). This metastable minimum is the one described by the Peierls theory at high temperature (i.e. stabilization of the the cumulene phase by temperature). As  $T$  approaches  $T_P$  from above, the free energy curvature at zero BLA is reduced, becomes zero at  $T = T_P$  and negative below, as it happens in a prototypical second order phase transition (see also Fig. S9 in the SI). However, this minimum is, by far, not the global minimum of the free energy curve that occurs at large finite BLA values of the order of  $\approx 0.1\text{\AA}$ . Even at temperatures as large as 1200 K, the quantum free energy calculation shows that polyyne is the most stable phase with an energy gain with respect to cumulene of  $\approx 6$  meV per atom. The transition between the two structures occurs at extremely high and unphysical temperatures (extrapolated to  $\approx 3500$  K within PBE0, see SI Sec. S2.5). Our calculation explains why only polyyne is always detected in experiments and not cumulene, even at very high temperatures.<sup>4,6,7,24–27</sup>

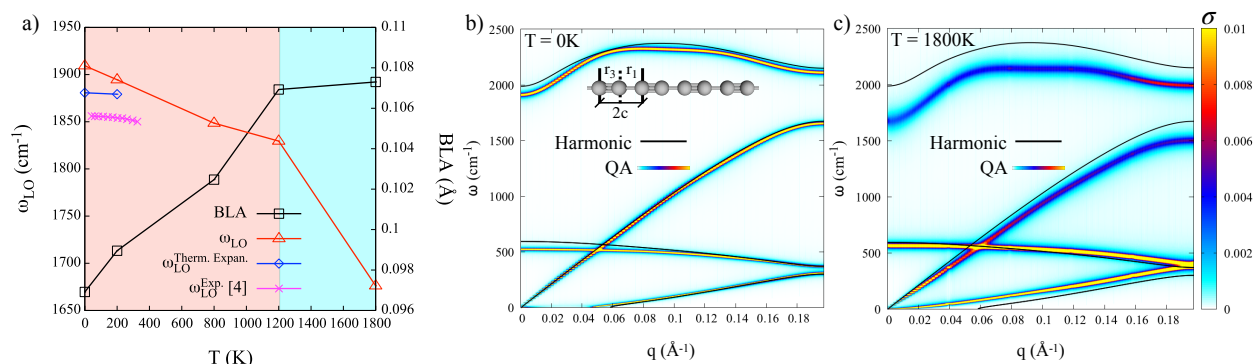


Figure 2: **Vibrational properties of polyyne.** a) Bond length alternation and longitudinal optical phonon frequency (including quantum anharmonic effects) for the polyyne phase as a function of temperature:  $\omega_{LO}^{\text{Exp.}}$ ,  $\omega_{LO}$  and  $\omega_{LO}^{\text{Therm. Expan.}}$  are the experimental<sup>4</sup> and theoretical longitudinal phonon frequencies at fixed and relaxed lattice parameters (for more details see Sec. S2.6 in the SI) b)-c) Harmonic (black solid line) and quantum anharmonic (color map) phonon dispersion relation of polyyne at  $T = 0$  K (c) and  $T = 1800$  K (d) The color bar represents the magnitude of the phonon cross-section  $\sigma$  (Eq. S7).

Finally, we remark that in a second order CDW phase transition, the magnitude of the order parameter (BLA) should decrease as temperature increases and, ultimately, becomes zero at and above the CDW transition. In the case of polyyne the opposite occurs, namely

1  
2  
3 the BLA *increases by increasing temperature* up to  $\approx 1200\text{K}$  (Fig. 2 (a)) and ultimately it  
4 saturates above 1200 K due to the occurrence of an unexpected insulator-to-metal transition  
5 driven by quantum anharmonic effects (see later). We underline that the results in Fig. 2  
6 (a) (black line) for the BLA have been obtained by performing the full quantum anharmonic  
7 optimization of the internal coordinates at fixed cell.  
8

9  
10  
11  
12  
13 The phonon dispersions of polyne are shown in Fig. 2 (b)-(c), both in the harmonic ap-  
14 proximation (black solid line) and by including dynamical effects in the anharmonic phonon  
15 spectral weight (color maps, see Sec. S2.1 of SI and Ref.<sup>30</sup> for more details). In the static  
16 case, quantum anharmonicity lowers the energy of the longitudinal optical mode (Fig. S6  
17 (a) ). However, dynamical effects in the phonon spectral weight enhance the quasiparticle  
18 energies with respect to the static case both of optical and acoustic modes, as shown in Fig. 2  
19 (b)-(c) (see also Sec. S2.3 in the SI). Finally, the dependence on temperature of the dynami-  
20 cal phonon frequency of the longitudinal optical Raman-active mode at fixed cell is reported  
21 in Fig. 2 (a) and in Tab. 1. The phonon frequency decreases linearly with temperature up  
22 to the insulator-to-metal transition at  $\approx 1200\text{ K}$ . At  $T = 0$  ( $T = 800\text{K}$ ) the blueshift of the  
23 Raman active mode due to quantum anharmonicity is  $\approx 77\text{ cm}^{-1}$  ( $\approx 137\text{ cm}^{-1}$ ), namely  
24 approximately 4% (7%) of the harmonic PBE0 phonon frequency.  
25  
26  
27  
28  
29  
30  
31  
32  
33  
34  
35  
36

37 In the 0 – 200 K temperature range, where experimental data are available,<sup>4</sup> we per-  
38 form the complete quantum anharmonic optimization of the crystal structure to account for  
39 the thermal expansion. Going from 0 to 200 K, Carbyne tends to contract by increasing  
40 temperature (see SI Sec. 2.6) which affects the temperature dependence of the longitudinal  
41 optical phonon frequency. If the (negative) thermal expansion is included, the behaviour  
42 of the longitudinal optical phonon frequency versus temperature is in good agreement with  
43 available experimental data, as shown in Fig. 2 (a).  
44  
45  
46  
47  
48  
49  
50  
51  
52

53 The zero temperature electronic structure and optical properties of carbyne in vacuum on  
54 the CAMB3LYP geometry are shown in Fig. 3 (a) and (b). As it can be seen, the CAMB3LYP  
55  
56  
57  
58  
59  
60

direct band-gap at zone border is very similar to the one obtained with self-consistent GW (evGW). The optical properties have been calculated using the Bethe-Salpeter equations on top of the evGW eigenvalues. In the absence of quantum anharmonicity, the lowest energy exciton is dark triplet at 2.27 eV, followed by a dark singlet state at 2.55 eV and the bright singlet state at 2.95 eV. The bright singlet exciton corresponds to optical transition across the direct band gap at zone border. However, given the importance of quantum anharmonic effects, a substantial renormalization of the optical gap and optical properties due to vibration occurs in polyyne. We evaluate the effect of quantum anharmonicity on the single particle gap by averaging the density of states over the SSCHA configurations in a 200 atoms polyyne supercell. At  $T = 0$ , the quantum anharmonic renormalization of the single particle gap is  $\approx -0.56$  eV ( $\approx 13\%$  of the evGW gap). This is shown in Fig. 3(b), where all the optical spectra are redshifted of the quantum anharmonic renormalization. Thus, we conclude that (i) the effect of quantum-anharmonicity are large and relevant on the optical spectra and (ii) the hybrid functional direct gap is in excellent agreement with Bethe-Salpeter and with that extrapolated from coupled cluster.<sup>4</sup>

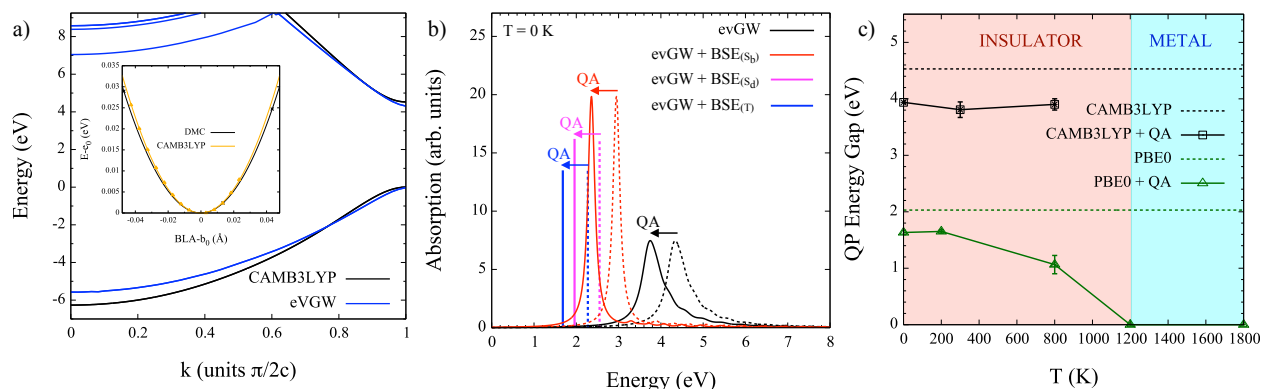


Figure 3: **Insulator to metal transition in polyyne.** a) Electronic structure of polyyne with different approximations for the electron-electron interaction. (b) Optical absorption spectra of carbyne in the Bethe Salpeter approximation on top of evGW with/without inclusion of quantum anharmonic (QA) effects. (c) Quasiparticle band gap in polyyne as a function of temperature computed both with PBE0 and CAMB3LYP functionals, displaying the occurrence of an insulator to metal transition at 1200 K with PBE0.

For what concerns the modeling of Carbyne inside the nanotube, the situation is some-

1  
2  
3 what more complicated as experimental details on the nanotube shape and transport char-  
4 acteristics are missing.<sup>47</sup> As a working hypothesis, we assume the nanotube to be semicon-  
5 ducting and to act as an effective dielectric environment. For what concerns the evGW  
6 and Bethe Salpeter calculations on top of the PBE0 geometry, they include the effect of  
7 the environment only on the structure but not on the optical spectrum, as they are carried  
8 out without explicitly including the nanotube. However, the reduction of the quasiparticle  
9 band gap due to the environment can be understood as a polarization effect<sup>49</sup> and therefore  
10 treated as an effective dielectric constant,<sup>50</sup> assuming not too strong overlap between the  $\pi$   
11 orbitals of the chain and nanotube. A quantitative estimate of the screening of the dielectric  
12 environment can be obtained by considering the difference between the evGW (3.21 eV) and  
13 PBE (0.93 eV) gaps in the PBE0 geometry, dividing this difference for a typical dielectric  
14 constant of an insulator ( $\epsilon_M = 3 - 4$ ) and adding it back to the PBE value. This procedure  
15 leads to direct single particle gaps of 1.5 – 1.69, slightly lower than the PBE0 gap of 2.03  
16 eV. This suggests that the PBE0 single particle gap is of the same order of magnitude as  
17 the one obtained in a typical dielectric environment.  
18  
19  
20  
21  
22  
23  
24  
25  
26  
27  
28  
29  
30  
31  
32

33 Even in this case, quantum-anharmonicity is large and leads to an additional suppression  
34 of the band-gap of 0.4 eV, only a factor of 2 smaller than the gap-enhancement found via  
35 evGW. However, the effects of quantum anharmonicity strongly increase with temperature.  
36 By assuming the evGW correction to the single particle gap to be temperature independent,  
37 as it is reasonable to think, we find that the effects of vibrations on the optical gap become  
38 dominant at high temperature and lead to a gap closure and a stabilization of a metallic  
39 distorted polyynic phase above  $T_{MI} \approx 1200$  K (Fig. 3 (c) ) in the presence of an external  
40 dielectric environment. This insulator-to-metal transition is then observable and will occur  
41 earlier the larger the dielectric constant of the nanotube. In vacuum the larger size of the  
42 gap pushes the insulator-metal transition to very large unphysical temperatures, as shown  
43 in Fig. 3 (c).  
44  
45  
46  
47  
48  
49  
50  
51  
52  
53  
54

55 The structural fingerprints of the metallic distorted phase are then a very weak temper-  
56  
57  
58  
59  
60

1  
2  
3 ature dependence in the BLA and an enhancement of the phonon softening of the optical  
4 Raman active mode as a function of temperature, as shown in Fig. 2 (a).  
5  
6  
7

8  
9 In this work, we have shown that the cumulene-to-polyyne phase transition occurs only  
10 at unphysically large temperatures, with a bond length alternation that *increases as temper-*  
11 *ature increases*. The finite-temperature effects of quantum anharmonicity, poorly explored  
12 in literature, are extremely large and strongly affect the structural and vibrational proper-  
13 ties as well as the optical absorption. The large band-gap renormalization due to quantum  
14 anharmonic effects leads to a completely unexpected insulator-to-metal transition at high  
15 temperature stabilising a metallic polyynic phase. The larger the environmental dielectric  
16 constant of the nanotube, the lower the temperature for the insulator-metal transition. The  
17 experimental synthesis of ultralong polyyne carbon chains<sup>3-5</sup> and temperature dependent  
18 optical measurements will allow for an experimental verification of this claim.  
19  
20  
21  
22  
23  
24  
25  
26  
27  
28  
29  
30

## 31 Acknowledgement

32  
33  
34 D. R. and M.C. acknowledge support from the ANR project ACCEPT (Grant No. ANR-  
35 19-CE24-0028). This work was granted access to the HPC resources of IDRIS, CINES and  
36 TGCC under the allocation 2021-A0100912417 made by GENCI. Computational resources  
37 were also provided by the CINECA award "ISCRA B" HP10BB2RVB (2019). D. R. thanks  
38 D. Varsano for fruitful discussion on the GW+BSE computations and A. Erba.  
39  
40  
41  
42  
43  
44  
45  
46

## 47 Supporting Information Available

48  
49 Supporting information accompanies this paper, containing detailed description of: Com-  
50 putational details, SSCHA details, static and dynamic anharmonic phonon spectra of car-  
51 byne, *evGW* electronic structure convergence, CAMB3LYP analysis of polyyne. Corre-  
52 spondence and requests for materials should be addressed to romanin@insp.jussieu.fr and  
53  
54  
55  
56  
57  
58  
59  
60

m.calandrabuonaura@unitn.it.

## References

- (1) Peierls, R. E. Quelques proprietes typiques des corps solides. *Ann. I. H. Poincare* **1935**, *5*, 177–222.
- (2) Gruner, G. *Density waves in solids*; CRC Press, 1994.
- (3) Shi, L.; Rohringer, P.; Wanko, M.; Rubio, A.; Waßerroth, S.; Reich, S.; Cambré, S.; Wenseleers, W.; Ayala, P.; et al. Electronic band gaps of confined linear carbon chains ranging from polyynes to carbyne. *Phys. Rev. Materials* **2017**, *1*, 075601.
- (4) Shi, L.; Rohringer, P.; Suenaga, K.; Niimi, Y.; Kotakoski, J.; Meyer, J. C.; Peterlik, H.; Wanko, M.; Cahangirov, S.; Rubio, A. et al. Confined linear carbon chains as a route to bulk carbyne. *Nature Materials* **2016**, *15*, 634–639.
- (5) Heeg, S.; Shi, L.; Poulikakos, L. V.; Pichler, T.; Novotny, L. Carbon Nanotube Chirality Determines Properties of Encapsulated Linear Carbon Chain. *Nano Lett.* **2018**, *18*, 5426–5431.
- (6) Chalifoux, W. A.; Tykwinski, R. R. Synthesis of polyynes to model the sp-carbon allotrope carbyne. *Nature Chemistry* **2010**, *2*, 967–971.
- (7) Agarwal, N. R.; Lucotti, A.; Fazzi, D.; Tommasini, M.; Castiglioni, C.; Chalifoux, W.; Tykwinski, R. R. Structure and chain polarization of long polyynes investigated with infrared and Raman spectroscopy. *J. Raman Spectrosc.* **2013**, *44*, 1398–1410.
- (8) da Silva Neto, E. H.; Aynajian, P.; Frano, A.; Comin, R.; Schierle, E.; Weschke, E.; Gyenis, A.; Wen, J.; Schneeloch, J.; Xu, Z. et al. Ubiquitous Interplay Between Charge Ordering and High-Temperature Superconductivity in Cuprates. *Science* **2014**, *343*, 393.

- 1  
2  
3 (9) Wilson, J.; Salvo, F. D.; Mahajan, S. Charge-density waves and superlattices in the  
4 metallic layered transition metal dichalcogenides. *Advances in Physics* **1975**, *24*, 117–  
5 201.  
6  
7  
8  
9  
10 (10) Xi, X.; Zhao, L.; Wang, Z.; Berger, H.; Forró, L.; Shan, J.; Mak, K. F. Strongly enhanced  
11 charge-density-wave order in monolayer NbSe<sub>2</sub>. *Nature Nanotechnology* **2015**, *10*, 765–  
12 769.  
13  
14  
15  
16  
17 (11) Chen, Y.; Ruan, W.; Wu, M.; Tang, S.; Ryu, H.; Tsai, H.-Z.; Lee, R.; Kahn, S.; Liou, F.;  
18 Jia, C. et al. Strong correlations and orbital texture in single-layer 1T-TaSe<sub>2</sub>. *Nature*  
19 *Physics* **2020**, *16*, 218–224.  
20  
21  
22  
23 (12) Calandra, M. Charge density waves go nano. *Nature Nanotechnology* **2015**, *10*, 737–738.  
24  
25  
26 (13) Zhang, K.; Liu, X.; Zhang, H.; Deng, K.; Yan, M.; Yao, W.; Zheng, M.; Schiwer, E. F.;  
27 Shimada, K.; Denlinger, J. D. et al. Evidence for a Quasi-One-Dimensional Charge  
28 Density Wave in CuTe by Angle-Resolved Photoemission Spectroscopy. *Phys. Rev. Lett.*  
29 **2018**, *121*, 206402.  
30  
31  
32  
33  
34  
35 (14) Zhou, J. S.; Bianco, R.; Monacelli, L.; Errea, I.; Mauri, F.; Calandra, M. Theory of the  
36 thickness dependence of the charge density wave transition in 1 T-TiTe<sub>2</sub>. *2D Materials*  
37 **2020**, *7*, 4.  
38  
39  
40  
41  
42 (15) Zhou, J. S.; Bianco, R.; Monacelli, L.; Errea, I.; Mauri, F.; Calandra, M. Anharmonicity  
43 and Doping Melt the Charge Density Wave in Single-Layer TiSe<sub>2</sub>. *Nano Lett.* **2020**, *7*,  
44 4809–4815.  
45  
46  
47  
48  
49 (16) Bianco, R.; Monacelli, L.; Calandra, M.; Mauri, F.; Errea, I. Weak Dimensionality  
50 Dependence and Dominant Role of Ionic Fluctuations in the Charge-Density-Wave  
51 Transition of NbSe<sub>2</sub>. *Phys. Rev. Lett.* **2020**, *125*, 106101.  
52  
53  
54  
55  
56  
57  
58  
59  
60

- 1  
2  
3 (17) Errea, I.; Calandra, M.; Mauri, F. Anharmonic free energies and phonon dispersions  
4 from the stochastic self-consistent harmonic approximation: Application to platinum  
5 and palladium hydrides. *Phys. Rev. B* **2014**, *89*, 064302.  
6  
7  
8  
9  
10 (18) Heimann, R. B.; Kleiman, J.; Salansky, N. M. A unified structural approach to linear  
11 carbon polytypes. *Nature* **1983**, *306*, 164–167.  
12  
13  
14 (19) Artyukhov, V. I.; Liu, M.; Yakobson, B. I. Mechanically Induced Metal-Insulator Tran-  
15 sition in Carbyne. *Nano Lett.* **2014**, *14*, 4224–4229.  
16  
17  
18  
19 (20) Torre, A. L.; Botello-Mendez, A.; Baaziz, W.; Charlier, J.-C.; Banhart, F. Strain-  
20 induced metal–semiconductor transition observed in atomic carbon chains. *Nat Com-*  
21 *mun* **2015**, *6*, 6636.  
22  
23  
24  
25 (21) Romdhane, F. B.; Adjizian, J.-J.; Charlier, J.-C.; Banhart, F. Electrical transport  
26 through atomic carbon chains: The role of contacts. *Carbon* **2017**, *122*, 92–97.  
27  
28  
29  
30 (22) Lin, Y.-C.; Morishita, S.; Koshino, M.; Yeh, C.-H.; Teng, P.-Y.; Chiu, P.-W.;  
31 Sawada, H.; Suenaga, K. Unexpected Huge Dimerization Ratio in One-Dimensional  
32 Carbon Atomic Chains. *Nano Lett.* **2017**, *17*, 494–500.  
33  
34  
35  
36 (23) Milani, A.; Barbieri, V.; Facibeni, A.; Russo, V.; Bassi, A. L.; Lucotti, A.; Tom-  
37 masini, M.; Tzirakis, M. D.; Diederich, F.; Casari, C. S. Structure modulated charge  
38 transfer in carbon atomic wires. *Sci Rep* **2019**, *9*, 1648.  
39  
40  
41  
42 (24) Malard, L. M.; Nishide, D.; Dias, L. G.; Capaz, R. B.; Gomes, A. P.; Jorio, A.;  
43 Achete, C. A.; Saito, R.; Achiba, Y.; Shinohara, H. et al. Resonance Raman study  
44 of polyynes encapsulated in single-wall carbon nanotubes. *Phys. Rev. B* **2007**, *76*,  
45 233412.  
46  
47  
48  
49 (25) Moura, L. G.; Malard, L. M.; Carneiro, M. A.; Venezuela, P.; Capaz, R. B.; Nishide, D.;  
50 Achiba, Y.; Shinohara, H.; Pimenta, M. A. Charge transfer and screening effects in  
51  
52  
53  
54  
55  
56  
57  
58  
59  
60

- 1  
2  
3 polyynes encapsulated inside single-wall carbon nanotubes. *Phys. Rev. B* **2009**, *80*,  
4 161401(R).  
5  
6  
7
- 8 (26) Fantini, C.; Cruz, E.; Jorio, A.; Terrones, M.; Terrones, H.; Lier, G. V.; Charlier, J.-  
9 C.; Dresselhaus, M. S.; Saito, R.; Kim, Y. A. et al. Resonance Raman study of linear  
10 carbon chains formed by the heat treatment of double-wall carbon nanotubes. *Phys.*  
11 *Rev. B* **2006**, *73*, 193408.  
12  
13  
14  
15  
16
- 17 (27) Andrade, N. F.; Vasconcelos, T. L.; Gouvea, C. P.; Archanjo, B. S.; Achete, C. A.;  
18 Kim, Y. A.; Endo, M.; Fantini, C.; Dresselhaus, M. S.; Filho, A. S. Linear carbon  
19 chains encapsulated in multiwall carbon nanotubes: Resonance Raman spectroscopy  
20 and transmission electron microscopy studies. *Carbon* **2015**, *90*, 172–180.  
21  
22  
23  
24  
25
- 26 (28) Bianco, R.; Errea, I.; Paulatto, L.; Calandra, M.; Mauri, F. Second-order struc-  
27 tural phase transitions, free energy curvature, and temperature-dependent anharmonic  
28 phonons in the self-consistent harmonic approximation: Theory and stochastic imple-  
29 mentation. *Phys. Rev. B* **2017**, *96*, 014111.  
30  
31  
32  
33
- 34 (29) Monacelli, L.; Errea, I.; Calandra, M.; Mauri, F. Pressure and stress tensor of com-  
35 plex anharmonic crystals within the stochastic self-consistent harmonic approximation.  
36 *Phys. Rev. B* **2018**, *98*, 024106.  
37  
38  
39  
40
- 41 (30) Monacelli, L.; Bianco, R.; Cherubini, M.; Calandra, M.; Errea, I.; Mauri, F. The  
42 stochastic self-consistent harmonic approximation: calculating vibrational properties  
43 of materials with full quantum and anharmonic effects. *J. Phys.: Condens. Matter*  
44 **2021**, *33*, 363001.  
45  
46  
47  
48  
49
- 50 (31) Giannozzi, P.; Baroni, S.; Bonini, N.; Calandra, M.; Car, R.; Cavazzoni, C.; Ceresoli, D.;  
51 Chiarotti, G. L.; Cococcioni, M.; Dabo11, I. et al. QUANTUM ESPRESSO: a modu-  
52 lar and open-source software project for quantum simulations of materials. *Journal of*  
53 *Physics: Condensed Matter* **2009**, *21*, 395502.  
54  
55  
56  
57  
58  
59  
60

- 1  
2  
3 (32) Giannozzi, P.; Andreussi, O.; Brumme, T.; Bunau, O.; Nardelli, M. B.; Calandra, M.;  
4 Car, R.; Cavazzoni, C.; Ceresoli, D.; Cococcioni, M. et al. Advanced capabilities for  
5 material modeling with Quantum ESPRESSO. *Journal of Physics: Condensed Matter*  
6 **2017**, *29*, 465901.  
7  
8  
9  
10  
11 (33) Dovesi, R.; Orlando, R.; Erba, A.; Zicovich-Wilson, C. M.; Civalleri, B.; Casassa, S.;  
12 Maschio, L.; Ferrabone, M.; Pierre, M. D. L.; D'Arco, P. et al. Crystal14: A program  
13 for the ab-initio investigation of crystalline solids. *International Journal of Quantum*  
14 *Chemistry* **2014**, *114*, 1287–1317.  
15  
16  
17  
18 (34) Dovesi, R.; Erba, A.; Orlando, R.; Zicovich-Wilson, C. M.; Civalleri, B.; Maschio, L.;  
19 R erat, M.; Casassa, S.; Baima, J.; Salustro, S. et al. Quantum-mechanical condensed  
20 matter simulations with CRYSTAL. *WIREs Comput Mol Sci.* **2018**, *8*, 1360.  
21  
22  
23 (35) Oliveira, D. V.; Laun, J.; Peintinger, M. F.; Bredow, T. Bsse-correction scheme for  
24 consistent gaussian basis sets of double- and triple-zeta valence with polarization quality  
25 for solid-state calculations. *Journal of Computational Chemistry* **2019**, *40*, 2364–2376.  
26  
27  
28 (36) Marini, A.; Hogan, C.; Gr uning, M.; Varsano, D. yambo: An ab initio tool for excited  
29 state calculations. *Computer Physics Communications* **2009**, *8*, 180.  
30  
31  
32 (37) Sangalli, D.; Ferretti, A.; Miranda, H.; Attaccalite, C.; Marri, I.; Cannuccia, E.;  
33 Melo, P.; Marsili, M.; Paleari, F.; Marrazzo, A. et al. Many-body perturbation the-  
34 ory calculations using the yambo code. *Journal of Physics: Condensed Matter* **2019**,  
35 *31*, 325902.  
36  
37  
38 (38) Rojas, H. N.; Godby, R. W.; Needs, R. J. Space-Time Method for Ab Initio Calculations  
39 of Self-Energies and Dielectric Response Functions of Solids. *Phys. Rev. B* **1995**, *74*,  
40 10.  
41  
42  
43 (39) Strinati, G. Application of the Green's functions method to the study of the optical  
44 properties of semiconductors. *Rivista del Nuovo Cimento* **1988**, *11*, 12.  
45  
46  
47  
48  
49  
50  
51  
52  
53  
54  
55  
56  
57  
58  
59  
60

- 1  
2  
3 (40) Bussi, G. Effects of the Electron–Hole Interaction on the Optical Properties of Materi-  
4 als: the Bethe–Salpeter Equation. *Physica Scripta* **2003**, *2004*, 141.  
5  
6  
7  
8 (41) Abdurahman, A.; Shukla, A.; Dolg, M. Ab initio many-body calculations on infinite  
9 carbon and boron-nitrogen chains. *Phys. Rev. B* **2002**, *65*, 115106.  
10  
11  
12 (42) Yang, S.; Kertesz, M. Bond Length Alternation and Energy Band Gap of Polyyne. *J.*  
13 *Phys. Chem. A* **2006**, *110*, 9771–9774.  
14  
15  
16  
17 (43) Jacquemin, D.; Femenias, A.; Chermette, H.; Ciofini, I.; Adamo, C.; André, J.-M.;  
18 Perpète, E. A. Assessment of Several Hybrid DFT Functionals for the evaluation of  
19 Bond Length Alternation of Increasingly Long Oligomers. *J. Phys. Chem. A* **2006**,  
20 *110*, 5952–5959.  
21  
22  
23  
24  
25  
26 (44) Peach, M. J. G.; Tellgren, E. I.; Salek, P.; Helgaker, T.; ; Tozer, D. J. Structural  
27 and Electronic Properties of Polyacetylene and Polyyne from Hybrid and Coulomb-  
28 Attenuated Density Functionals. *J. Phys. Chem. A* **2007**, *111*, 11930–11935.  
29  
30  
31  
32  
33 (45) Mostaani, E.; Monserrat, B.; Drummond, N. D.; Lambert, C. J. Quasiparticle and  
34 excitonic gaps of one-dimensional carbon chains. *Phys. Chem. Chem. Phys.* **2016**, *18*,  
35 14810–14821.  
36  
37  
38  
39  
40 (46) Ramberger, B.; Kresse, G. New insights into the 1D carbon chain through the RPA.  
41 *Phys. Chem. Chem. Phys.* **2021**, *23*, 5254.  
42  
43  
44  
45 (47) Experimentally it is unclear if the double wall nanotubes into which carbyne is grown  
46 are insulating or metallic as the chains are grown inside the inner tubes at very high  
47 temperature from filled carbonaceous precursors.  
48  
49  
50  
51 (48) Shi, L.; Rohringer, P.; Wanko, M.; Rubio, A.; Waßerroth, S.; Reich, S.; Cambré, S.;  
52 Wenseleers, W.; Ayala, P.; Pichler, T. Electronic band gaps of confined linear carbon  
53 chains ranging from polyyne to carbyne. *Phys. Rev. Materials* **2017**, *1*, 075601.  
54  
55  
56  
57  
58  
59  
60

- 1  
2  
3 (49) Neaton, J. B.; Hybertsen, M. S.; Louie, S. G. Renormalization of Molecular Electronic  
4 Levels at Metal-Molecule Interfaces. *Phys. Rev. Lett.* **2006**, *97*, 216405.  
5  
6  
7  
8 (50) Nugraha, A. R. T.; Saito, R.; Sato, K.; Araujo, P. T.; Jorio, A.; Dresselhaus, M. S.  
9 Dielectric constant model for environmental effects on the exciton energies of single  
10 wall carbon nanotubes. *Appl. Phys. Lett.* **2010**, *97*, 091905.  
11  
12  
13  
14  
15  
16  
17  
18  
19  
20  
21  
22  
23  
24  
25  
26  
27  
28  
29  
30  
31  
32  
33  
34  
35  
36  
37  
38  
39  
40  
41  
42  
43  
44  
45  
46  
47  
48  
49  
50  
51  
52  
53  
54  
55  
56  
57  
58  
59  
60